Delft University of Technology

Psychoacoustic Analysis of the Noise Emissions from the Airbus A320 Aircraft Family and its Nose Landing Gear System

Merino-Martinez, Roberto; Besnea, Irina; Hoff, Bieke von den; Snellen, Mirjam

Important note
To cite this publication, please use the final published version (if applicable).
Please check the document version above.

Psychoacoustic Analysis of the Noise Emissions from the Airbus A320 Aircraft Family and its Nose Landing Gear System

Roberto Merino-Martínez [*], Irina Besnea [†], Bieke von den Hoff [‡], and Mirjam Snellen [§]

Delft University of Technology, Kluyverweg 1, 2629 HS Delft, the Netherlands

This manuscript presents a psychoacoustic analysis of the noise emissions from the Airbus A320 aircraft family, with a special focus on the tonal noise emitted by its nose landing gear (NLG) system. The study is based on microphone array measurements of aircraft flyovers under operational conditions performed next to Amsterdam Airport Schiphol. It was found that the NLG system is a dominant tonal noise source for all aircraft subtypes measured (A319, A320, A320*neo*, A321, and A321*neo*) around 1700 Hz. The magnitude of the tonal noise observed was strongly correlated with the aircraft velocity, whereas the tonal frequency remained relatively constant. A preliminary psychoacoustic analysis between the different aircraft subtypes showed that, on average, the *neo* versions presented higher metric values for effective perceived noise level (EPNL), psychoacoustic annoyance, and loudness but lower tonality than their older *ceo* counterparts. However, given the low number of *neo* samples available in this study, no strong conclusion can be drawn from this analysis. Overall, the A321 aircraft measured presented lower average values for all noise metrics evaluated than the A320 ones, despite being larger and heavier. These claims will be evaluated in upcoming dedicated psychoacoustic listening experiments.

I. Introduction

Aircraft noise emissions negatively affect the well-being and living environment of millions of people in the vicinity of airports. Noise exposure has even been related to harmful long-term health effects, such as cardiovascular diseases or hearing problems [1, 2]. As a result, ever-stricter environmental noise regulations limit the capacity of airports, causing substantial loss of revenue [3, 4]. Therefore, obtaining effective reductions in aircraft noise emissions and noise exposure around airports is one of the main challenges of the aeronautical industry nowadays [5, 6].

During the last decades, the noise levels generated by turbofan engines have been considerably reduced by increasing their bypass ratio and by the implementation of noise-reduction technologies, such as acoustic lining [7]. Thus, the relative importance of airframe noise within the total aircraft noise emissions has considerably increased [8], especially during the approach stage when the engines typically operate at lower rotational speeds. Thus, airframe noise is now considered a future lower bound to aircraft noise emissions [9]. Therefore, identifying the noisiest aircraft elements is essential to obtain detailed information on their characteristics to devise effective noise-reduction measures [10] and achieve more accurate noise prediction models for better planning around airports [11].

Out of all the airframe components, the landing gear (LG) system is considered the dominant noise source during the approach stage for modern commercial aircraft [8, 12, 13]. The LG system consists of complex bluff-body structures (e.g. struts, links, wheels, fairings, cavities, etc.) of different sizes that are (typically) not acoustically optimized [14]. Hence, the sound generation mechanisms and noise emissions of this system are relatively complex. They typically present a combination of tonal noise, generated by cavity resonances [15, 16] and Aeolian tones due to flow separation and vortex shedding [17], as well as broadband noise, mainly caused by the interaction of the LG system with turbulent flow. Nevertheless, the contribution of the Aeolian tones to the overall noise levels is usually negligible and their tonal frequencies are generally considerably lower (around 100 Hz) than those corresponding to cavity noise [18].

In particular, several experimental studies featuring aircraft flyover measurements reported that the nose landing gear (NLG) system of certain commercial aircraft types emits a very prominent tonal noise component [9, 14, 19–22]. The noise-generation mechanism is likely to be the interaction of the grazing turbulent airflow over pin-hole cavities within the structure of the NLG [9, 17, 22]. In general, parasitic noise sources (e.g. pin-hole cavities, anti-ice vents [23], or fuel

---

[*]Assistant professor, Aircraft Noise and Climate Effects section, Faculty of Aerospace Engineering. Email: r.merinomartinez@tudelft.nl
[†]PhD candidate, Aircraft Noise and Climate Effects (ANCE), i.besnea@tudelft.nl
[‡]PhD candidate, Aircraft Noise and Climate Effects (ANCE), b.vondenhoff@tudelft.nl
[§]Full professor, Aircraft Noise and Climate Effects (ANCE), m.snellen@tudelft.nl

overpressure ports [9, 24, 25]) are rarely present in scaled-down aeroacoustic wind tunnel experiments or computational simulations due to the lack of detail required to accurately model the small-scale components generating the noise emissions [24]. Consequently, semi-empirical aircraft noise prediction models [26–28] based on these approaches do not normally include parasitic noise estimations in their calculations [22]. Nevertheless, the contribution of these tonal noise sources can be perceived in cruise configuration [24] and can even dominate the noise signature during landing [9], especially when considering that the LG doors start opening at a horizontal distance of approximately 10 km to touchdown (corresponding to altitudes of only 500 m approximately), hence affecting large numbers of residents. Moreover, sounds with strong tonal components are perceived by the human ear as more annoying than a broadband sound with the same sound pressure level, L_p [29–32].

The present study focuses on the NLG tonal emissions of the Airbus A320 family, including different aircraft subtypes, such as the A319, A320, and A321, as well as their *neo* (referring to *new engine option*) upgraded versions developed during the last few years. With more than 10,000 aircraft delivered, the Airbus A320 family is particularly relevant for aircraft noise emissions around airports, as this is currently the world's most popular single-aisle aircraft family, with approximately a 60% market share [33]. In addition, previous studies [13, 22, 30] have reported particularly strong tonal noise emissions generated at the NLG system of aircraft from the A320 family. Such a tone is typically present at frequencies around 1700 Hz and can protrude more than 10 dB from the surrounding broadband noise [22]. The main improvements of the *neo* versions with respect to their older counterparts (usually referred to as *ceo, current engine option*) correspond to the engines, which are more fuel-efficient and expected to be quieter, and some aerodynamic enhancements, such as sharklet wingtips [33]. The design of the LG system, on the other hand, remains essentially constant across the A320 family variants, mostly to minimize operational complexities. Hence, the LG noise signature of the different subtypes of the A320 family is expected to be similar. However, the relative importance of the LG noise contribution and the prominence of the tonal noise components would vary depending on the other noise sources present on board. In the following discussions, and unless explicitly stated, the *ceo* versions are denoted as the general subtype, i.e. A320*ceo* is referred to as simply A320.

Since, in general, newer aircraft are subjected to stricter noise certification values, they are expected to cause lower noise annoyance to the population around airports. As an example, Fig. 1a presents the effective perceived noise level (EPNL) values for certification at the approach measurement point for the aircraft considered in this study, organized by their year of first flight. In particular, the *neo* versions of the A320 and A321 aircraft do have lower certification EPNL values than their *ceo* counterparts. Differences within the same aircraft subtype are due to the different turbofan engines. Nevertheless, there are some concerns regarding the use of conventional sound metrics, such as EPNL, to assess annoyance, since they fail to capture important sound characteristics that affect perception [34, 35]. In fact, despite reporting decreasig noise levels for conventional sound metrics recorded around Amsterdam Airport Schiphol (AAS) in the Netherlands [36–39], the number of complaints has, in general, increased over time. Ongoing research suggests the use of state-of-the-art perception-based sound metrics to overcome this limitation [40, 41].

The same trend is reflected in Fig. 1b where the average number of complaints per *neo* flight is lower than that for the *ceo* counterparts. This is, however, not true for the year 2020 which marks the introduction of A321*neo* flights to AAS. Nevertheless, due to the COVID-19 pandemic and the substantial decrease in global air traffic associated with it, the year 2020 might not have been particularly representative of community noise assessment. The data presented in Fig. 1b was obtained from the yearly reports of the Bewoners Aanspreekpunt Schiphol (BAS) association (in English: Residents Contact Point Schiphol) [36–39], which link the individual noise complaints received to specific flights and aircraft types.

The current manuscript is based on experimental acoustic field measurements of aircraft within the Airbus A320 family flying under operational conditions at Amsterdam Airport Schiphol (AAS). These acoustic measurements are analyzed in terms of conventional sound metrics (e.g. EPNL) as well as perception-based sound quality metrics (SQMs) [40, 45], see section III.B. In particular, the noise emissions and expected psychoacoustic annoyance of the newer models (*neo* versions) are compared to those of their older counterparts (*ceo* versions). Special focus is placed on assessing the tonal noise emissions of the NLG system given their high relevance for this aircraft type [13, 22, 30], and for the aforementioned future airframe noise lower bound. The microphone array employed for the field experiments combined with acoustic imaging algorithms enables the visualization of sound and the separate acoustic and psychoacoustic analysis of the noise emissions generated by the NLG [46, 47].

The manuscript is structured as follows. Section II describes the experimental setup employed for the aircraft flyover measurements. Section III explains the acoustic imaging method used on the recorded acoustic data, as well as the SQMs employed within the analysis. The main results obtained are discussed in Sec. IV, whereas the conclusions are drawn in Sec. V.
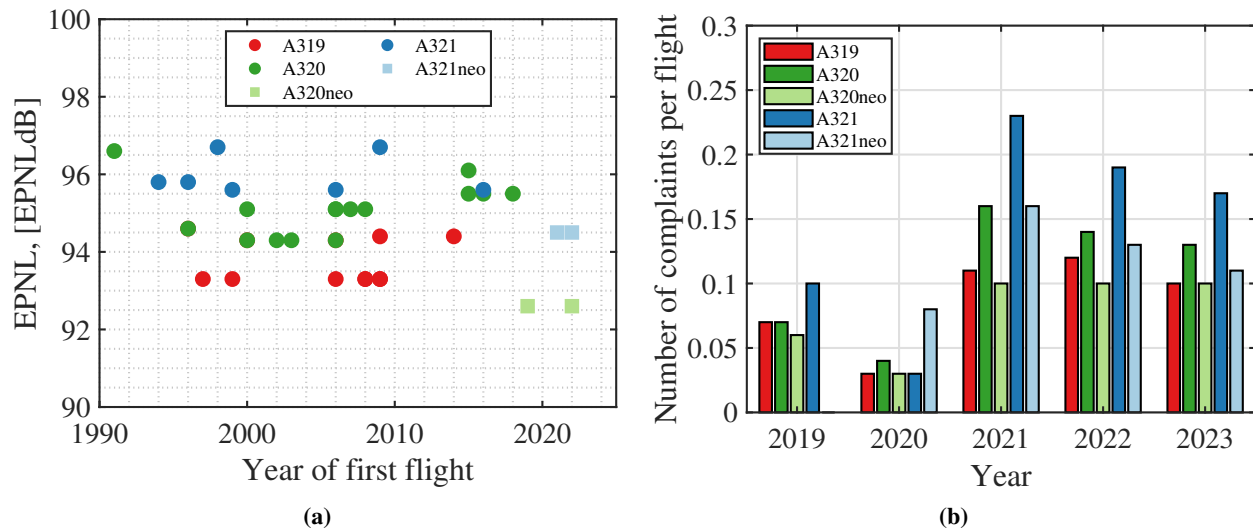
2

(a)

(b)

Fig. 1 **(a) Certification Effective Perceived Noise Levels (EPNL) values for each A320 aircraft flyover considered in this study grouped by subtype and ordered by the year of the first flight. These EPNL values correspond to the approach phase and were averaged over the different EASA variants. Data extracted from [42–44]. (b) Average number of complaints per flight at Amsterdam Airport Schiphol (AAS) for each A320 aircraft subtype throughout the years. Data extracted from [36–39].**

II. Experimental setup

The acoustic data was acquired at Amsterdam Airport Schiphol (AAS) through three separate measurement campaigns. The aircraft flyovers were measured during their final approach phase using a microphone array consisting of 60* PUI Audio POM-2735P-R analog condenser microphones [48] following an Underbrink 8-arm spiral distribution with a 4-m diameter (see Fig. 2(a)). The microphones have a sensitivity of -35 ± 2 dB (ref. 1 V/Pa) and a frequency range of 20 Hz to 25 kHz. The sampling frequency employed was 50 kHz. The array was placed north of the Zwanenburgbaan runway (18C), 640 m away from the runway threshold (see orange marker in Fig. 2(b)) to limit background noise (e.g. road traffic noise) while measuring as close as possible to the runway for achieving higher signal-to-noise ratios. Measuring so close to the runway threshold, however, implies that the operational and sound propagation conditions would vary compared to local communities around airports located further away. To attenuate sound reflections, the microphones were placed over a 15-mm layer of [49] Flamex Basic acoustic-absorbing foam. For the psychoacoustic analysis, one of the central microphones was selected, see red marker in Fig. 2(a).

A total of 38 aircraft flyovers from the Airbus A320 family were measured, out of which only four belonged to the upgraded *neo* versions. The main characteristics of each aircraft subtype are gathered in Table 1. Overall, the airframe of the different subtypes mostly varies in terms of fuselage length and number of passengers, with, consequently, higher maximum take-off weight (MTOW) and maximum thrust for higher subtype numbers. Furthermore, the *neo* versions are equipped with turbofan engines that have a larger fan diameter than their *ceo* predecessors, namely the CFMI LEAP-1A for the A320*neo* and the Pratt & Wittney PW1100G geared turbofan for the A321*neo*.

The aircraft flight paths were estimated from the Automatic Dependent Surveillance-Broadcast (ADS-B) data collected from OpenSky's database [51]. Since the ADS-B data is sampled every second, the velocity and altitude need to be interpolated to match the exact timestamps of the recorded acoustic data, which has a higher sampling rate. The aircraft velocity V and altitude h are then extracted at the overhead time of the aircraft, i.e., when the aircraft is overhead of the array (corresponding to an emission angle $\theta = 90°$, where $\theta = 0°$ corresponds to upstream and $\theta = 180°$ downstream). The overhead time is determined by correlating the latitude and longitude coordinates of the microphone array with the aircraft's position from the ADS-B data. Afterward, the (interpolated) velocity and the altitudes are evaluated for a 10 s interval centered at the overhead time to ensure that the glide slope remains approximately at $3°$. An overview of the distribution of the aircraft velocities overhead is provided in Fig. 3 as a boxplot, with values ranging from 53 m/s to 78.3 m/s (corresponding to Mach numbers M between 0.16 and 0.23). The estimated heights overhead

---

*Technically, the array consisted of 64 microphones, but four of them were found to be defective and are, thus, excluded from the analysis.
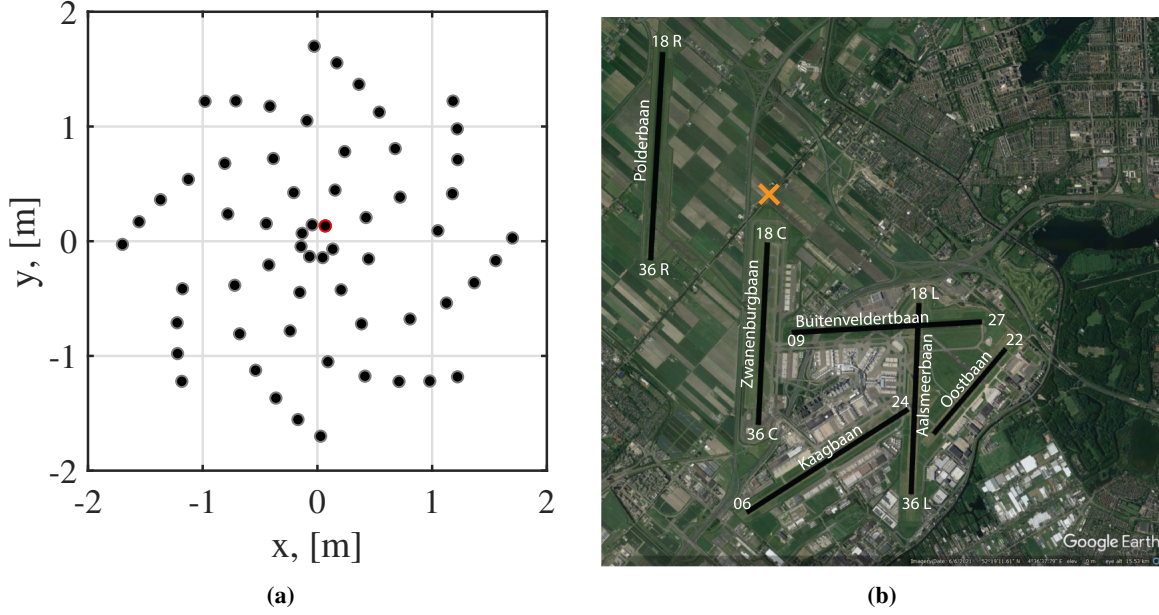
(a)

(b)

Fig. 2   (a) Microphone array configuration composed of 60 microphones. The red marker denotes the microphone employed for the psychoacoustic analysis. (b) Measurement location at Amsterdam Airport Schiphol (denoted by an orange marker). The runways are highlighted by the black lines.

Table 1   Main characteristics of the aircraft subtypes within the Airbus A320 family considered for this study [50].

Aircraft type	A319*ceo*	A320*ceo*	A320*neo*	A321*ceo*	A321*neo*
Measured aircraft	12	15	2	7	2
Wingspan, [m]	35.8	35.8	35.8	35.8	35.8
Fuselage length, [m]	33.84	37.57	37.57	44.51	44.51
Engine type	IAE V2500/CFM56	IAE V2500/CFM56	LEAP-1A	IAE V2500/CFM56	PW1100G
Fan diameter, [m]	1.61/1.73	1.61/1.73	1.98	1.61/1.73	2.06
Max Thrust, [kN]	120	120	120.6	142.34	147.28
MTOW, [t]	75.5	78	79	93.5	97
Number of passengers	160	180	180	220	244

ranged from 38.1 m to 99.1 m, with mean values of 62.3 m. To enable a fairer comparison between different flyovers and to provide acceptable sound levels for upcoming listening experiments, all the flyover recordings were scaled to a reference altitude overhead of 1000 m by applying a spherical spreading correction to the time signals of the sound pressures $p(t)$:

$$p_{\text{scaled}}(t) = p_{\text{original}}(t)\ \frac{h_{original}}{1000\,\text{m}}, \tag{1}$$

which is equivalent to a sound pressure level L_{p} correction of:

$$L_{\text{p,scaled}}(t) = L_{\text{p,original}}(t) + 20\ \log_{10}\left(\frac{h_{original}}{1000\,\text{m}}\right). \tag{2}$$

Therefore, the applied correction corresponded to reductions in the overall L_{p} values between 20.1 and 28.4 dB. This scaling, however, poses some limitations since given the differences in altitude and aircraft velocity, sound propagation phenomena, such as the Doppler effect, will vary per aircraft flyover.
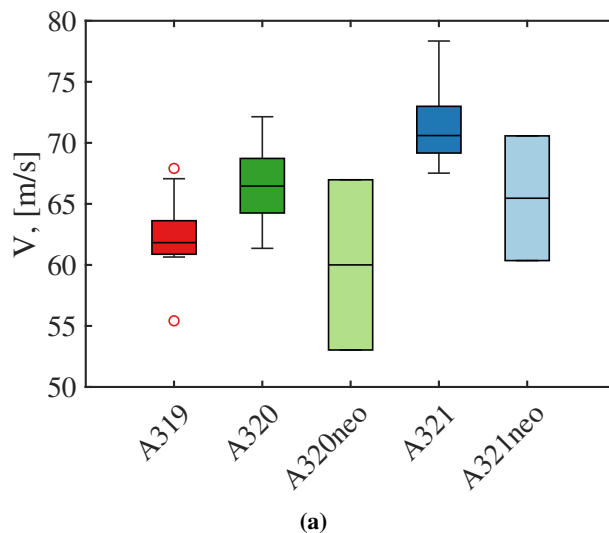
4

(a)

Fig. 3   Boxplot representing the aircraft velocity overhead per aircraft subtype. On each box, the central mark is the median, the edges of the box are the 25th and the 75th percentiles, and the whiskers extend to the most extreme data points. The outliers are plotted individually as red circles.

Meteorological data was collected to account for atmospheric attenuation. This data is recorded by the Royal Dutch Meteorological Institute (KNMI) [52] every hour, hence interpolation is necessary to estimate the parameters at the recording time of the acoustic signal. The parameters considered from the KNMI data are wind speed, wind direction, relative humidity, pressure, and temperature. While previous research showed that weather conditions are responsible for approximately 2 dBA level variability at most [53], the conditions during the measurement campaigns satisfied the ICAO atmospheric conditions for noise certification to increase comparability [54].

III. Methodology

A. Acoustic imaging method

The acoustic data recorded by the microphone array was post-processed using functional beamforming (FUNBF) [55] to visualize the main noise sources on board for each aircraft flyover. FUNBF provides lower sidelobe levels and improved array spatial resolution, without increasing the array's performance in separating closely located sources, compared to the conventional frequency domain beamforming (CFDBF) method. Essentially, this technique raises the autopowers of the CFDBF source map to the power of an exponent parameter ν and the cross-spectral matrix (CSM) to the inverse of this power $1/\nu$ to maintain the source levels. For this study, the value of ν was selected to be 8 after performing a sensitivity analysis [20, 56]. A scan grid placed at a distance from the array plane equal to the aircraft altitude overhead was employed. The scan grid spanned 50 m in the spanwise direction and 120 m in the streamwise direction to visualize different emission angles. A grid spacing between neighboring scan grid points of 1 m was used, providing a total of 6171 scan grid points. For the acoustic imaging analysis, a time interval of 0.123 s centered at the overhead time was employed and the frequency spectra were obtained following Welch's method [57] using a block length of 4096 samples (0.08 s), a Hanning windowing function and 50% data overlap, providing a frequency resolution Δf of 12.2 Hz.

Since the focus of this manuscript lies in the psychoacoustic investigation of the A320 subtypes, acoustic imaging is only conducted here to confirm the dominance of the NLG noise for the one-third-octave band centered at 1600 Hz. The NLG noise emissions could be isolated by integrating the FUNBF source maps around a region of interest [13, 21, 22], but this analysis is less relevant for the overall psychoacoustic annoyance experienced on the ground.

5

B. Sound quality metrics

Sound Quality Metrics (SQMs) describe the subjective perception of sound by human hearing, unlike the L_p metric, which quantifies the purely physical magnitude of sound based on the pressure fluctuations. Previous studies [32, 41] showed that these metrics better capture the auditory behavior of the human ear compared to conventional sound metrics typically employed in noise assessments. The five most commonly-used SQMs [40] are:

- Loudness (N): Subjective perception of sound magnitude corresponding to the overall sound intensity [58].
- Tonality (K): Measurement of the perceived strength of unmasked tonal energy within a complex sound [29].
- Sharpness (S): Representation of the high-frequency sound content [59].
- Roughness (R): Hearing sensation caused by sounds with modulation frequencies between 15 Hz and 300 Hz [60].
- Fluctuation strength (FS): Assessment of slow fluctuations in loudness with modulation frequencies up to 20 Hz, with maximum sensitivity for modulation frequencies around 4 Hz [61].

These five SQMs were calculated for each aircraft flyover recording and their 5% percentile values were considered (hence the "5" subindex henceforth), representing the value of each SQM exceeded 5% of the total recording time. These 5% percentile values were then combined into a single global psychoacoustic annoyance (PA) metric following the model outlined by Di *et al.* [62].

All the SQMs, the PA metric, as well as the conventional sound metrics (L_p, EPNL, etc.) were computed using the open-source MATLAB toolbox SQAT (Sound Quality Analysis Toolbox) v1.1 [40, 45]. The GitHub repository of the toolbox can be found in [63].

IV. Results and discussion

A. Acoustic analysis

As a preliminary comparison of the noise signatures within the Airbus A320 family, Fig. 4 depicts five spectrograms for a representative flyover of each A320 subtype. All spectrograms have a time step of 0.1 s and a frequency step of 10 Hz. All sound pressure levels correspond to the scaled aircraft altitude of 1000 m, see Sec. II. As reported in previous studies, a strong tone around 1700 Hz attributed to the NLG is observed in all cases, which follows the typical Doppler-shift curve due to the aircraft motion. The time overhead ($t = 0$ s) over the selected microphone is indicated with a vertical dashed blue line and the tonal frequency at that moment is highlighted with a green circle marker. A first comparison between the different spectrograms shows that the *neo* versions of the A320 and A321 subtypes (Figs. 4(c) and (e), respectively) present considerably higher noise levels for frequencies above 3 kHz, despite being newer aircraft and flying at slightly lower velocities. The frequency and L_p values of the NLG tone are similar for all the cases shown in Fig. 4: around 1700 Hz and between 52-54 dB, respectively.

This fact can be observed in a better way in Fig. 5, where the measured frequency spectra overhead for the A320 and A321*ceo* versions are compared to their *neo* counterparts. For these particular flyovers, the NLG tones seem more prominent (due to the lower broadband noise around them) for both A321 aircraft. Both *neo* versions present consistently higher noise levels for frequencies higher than 3 kHz, as aforementioned when discussing the spectrograms in Fig.. 4, but slightly lower broadband noise levels for frequencies below that value. The most likely explanation for these discrepancies is the different engines between each aircraft. For the specific aircraft compared in Fig. 5, the A320 aircraft was equipped with two IAE V2500-A1 turbofan engines, the A320*neo* had two CFMI LEAP-1A26, the A321 had two IAE V2533-A5, and the A321*neo* two Pratt & Whitney PW1133G. Additional flyover measurements of aircraft equipped with other types of engines showed similar trends.

The sources of the noise emissions observed in the spectrograms can be identified by analyzing the acoustic source maps. Figure 6 depicts the FUNBF acoustic source maps for the same A321*neo* flyover discussed in Figs. 4(e) and 5(b) for three different emission angles corresponding to $\theta \approx 53°$, $90°$, and $127°$. The results correspond to a one-third-octave frequency band centered at 1600 Hz, except for the case with $\theta \approx 53°$ (Fig. 6(a)), which corresponds to 2000 Hz, due to the Doppler shift. It can be observed that the source of the tonal noise corresponds indeed to the NLG system and that the NLG noise is particularly prominent at the emission angles of 53° and 127° (Figs. 6(a) and (c), respectively). For the time overhead ($\theta \approx 90°$, Fig. 6(b)), the engines also contribute substantially to the overall noise levels, as well as a small source around the tail of the aircraft that could perhaps be attributed to a cavity present in the auxiliary power unit (APU) exhaust outlet or an air conditioning outflow valve. The main landing gear (MLG) may also contribute to the noise levels observed next to the engines, but the array's spatial resolution is insufficient to separate its contribution, For the source maps presented in this paper, the altitude scaling of the audio files aforementioned in Sec. II was not applied.

The acoustic source maps included in Fig. 7 present the noise emissions of the same A321*neo* flyover from Fig. 6
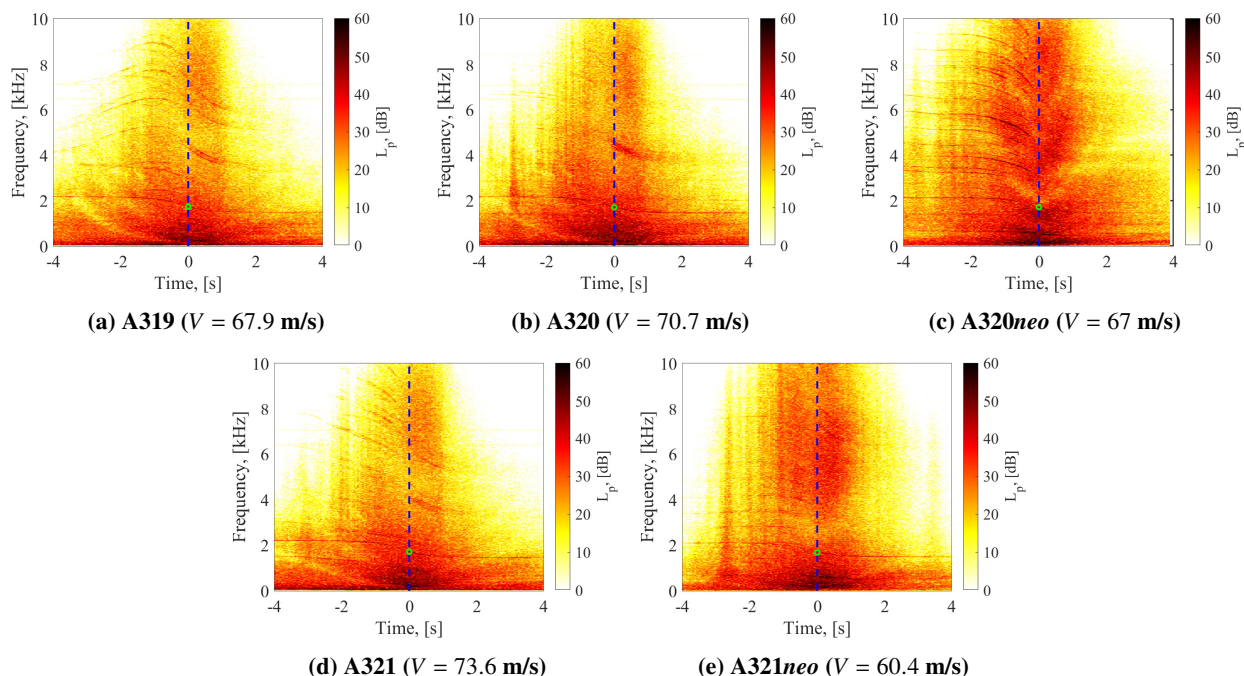
(a) A319 (V = 67.9 **m/s**)   **(b) A320** (V = 70.7 **m/s**)   **(c) A320***neo* (V = 67 **m/s**)

(d) A321 (V = 73.6 **m/s**)   **(e) A321***neo* (V = 60.4 **m/s**)

Fig. 4   Exemplary spectrograms of an aircraft flyover of each aircraft subtype. The aircraft velocities V overhead are specified in the captions of each subfigure. The time overhead is denoted by the vertical dashed blue line and the green circles denote the NLG tone at that moment.
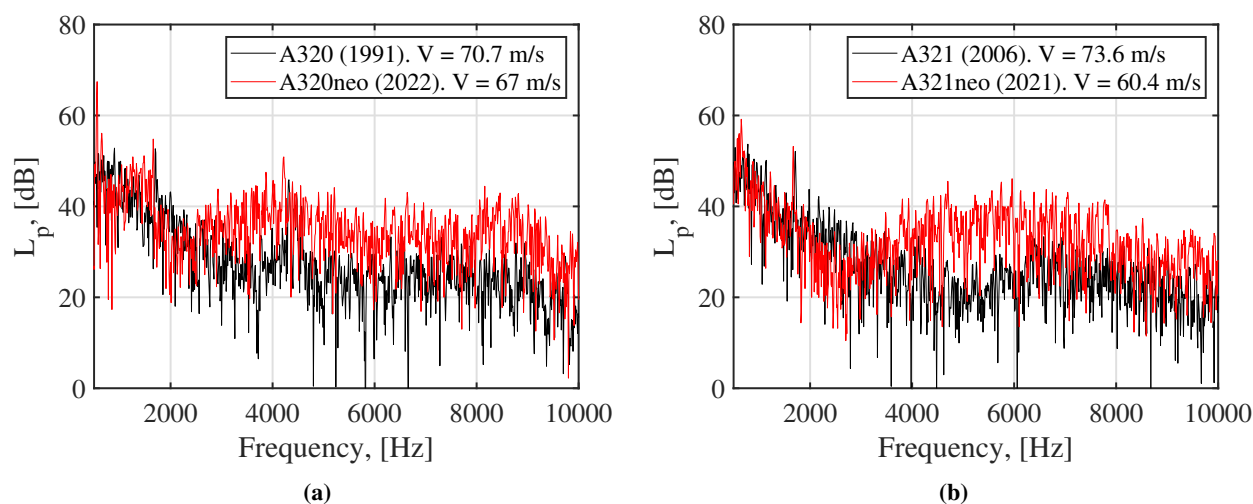

(a)   **(b)**

Fig. 5   Comparison between the frequency spectra measured overhead for exemplary flyovers of the *ceo* and *neo* versions of (a) A320 and (b) A321 aircraft.

but now for different one-third-octave frequency bands (1000 Hz, 3150 Hz, and 4000 Hz, respectively). The turbofan engines are the dominant noise source for all these frequency bands (and others not shown in this paper). For the one-third-octave frequency band centered at 1 kHz (Fig. 7(a)), extended noise sources along the wings can be observed as well, probably due to the extended high-lift devices during the approach phase.

For comparison purposes, Fig. 8 contains the acoustic source maps for the A321*ceo* discussed in Figs. 4(d) and 5(b) for some of the one-third-octave frequency bands discussed above (1600 Hz, 3150 Hz, and 4000 Hz) and for an emission angle of $\theta \approx 90°$. For the case of 1600 Hz (Fig. 8(a)), the noise sources corresponding to the turbofan engines seem
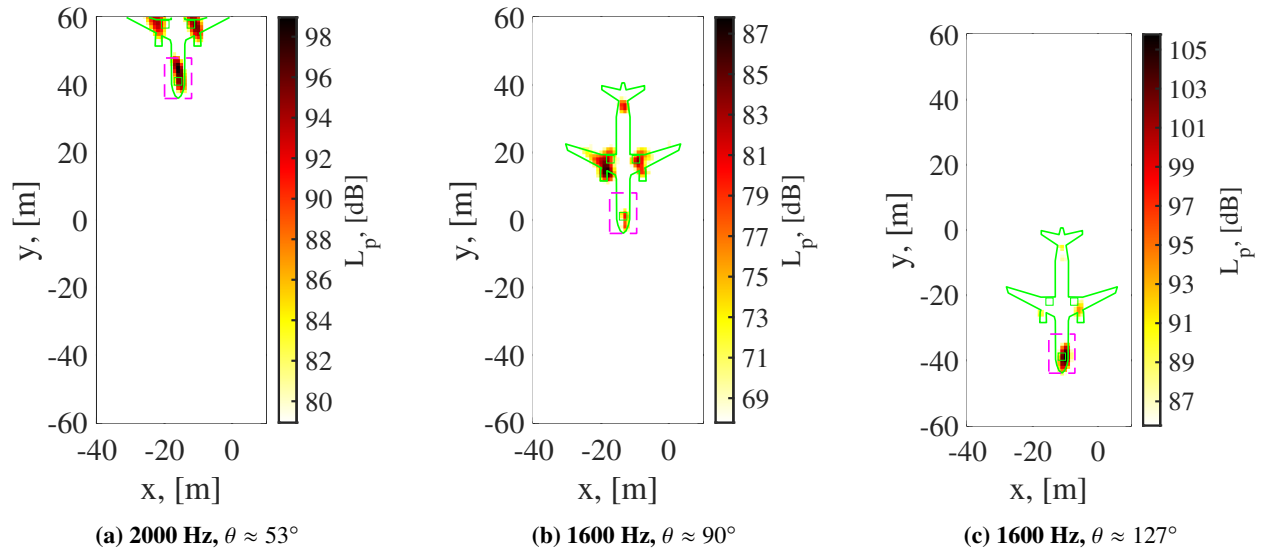
7

Fig. 6 **Functional beamforming acoustic source plots for an Airbus A321*neo* flyover with an aircraft velocity overhead of** $V = 60.4$ **m/s. The results correspond to different emission angles** θ**. Subfigure (a) corresponds to a one-third-octave frequency band centered at 2000 Hz (due to the Doppler shift), whereas subfigures (b) and (c) correspond to 1600 Hz. The aircraft silhouette is depicted as a green line with the landing gear wheels denoted with squares.**

Fig. 7 **Functional beamforming acoustic source plots for an Airbus A321*neo* flyover with an aircraft velocity overhead of** $V = 60.4$ **m/s for different one-third-octave frequency bands. The aircraft silhouette is depicted as a green line with the landing gear wheels denoted with squares.**

8

(a) 1600 Hz **(b) 3150 Hz** **(c) 4000 Hz**

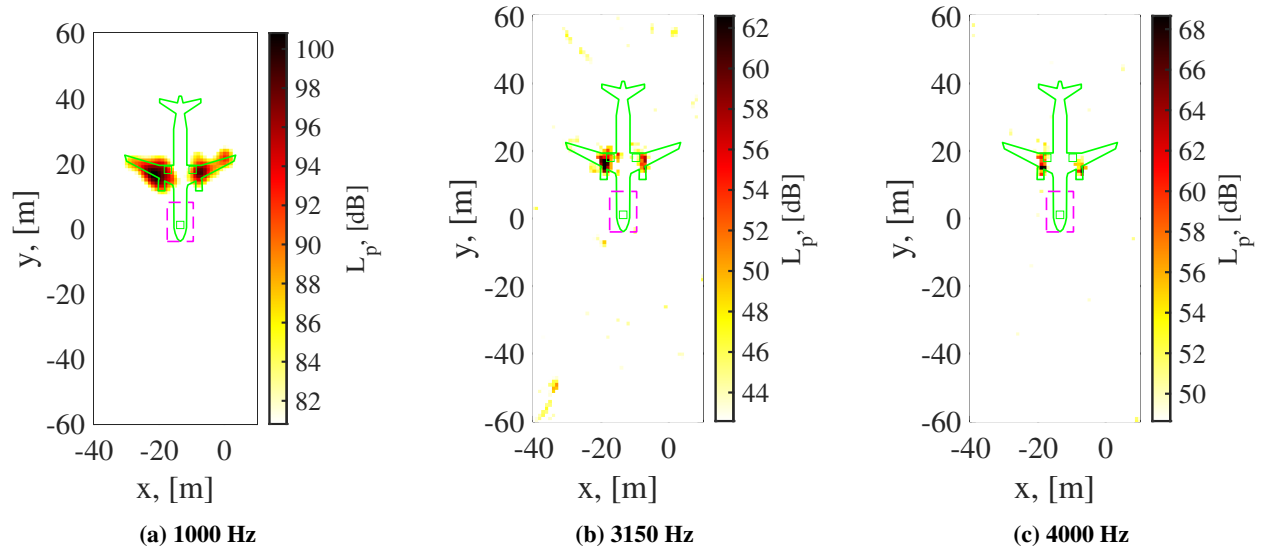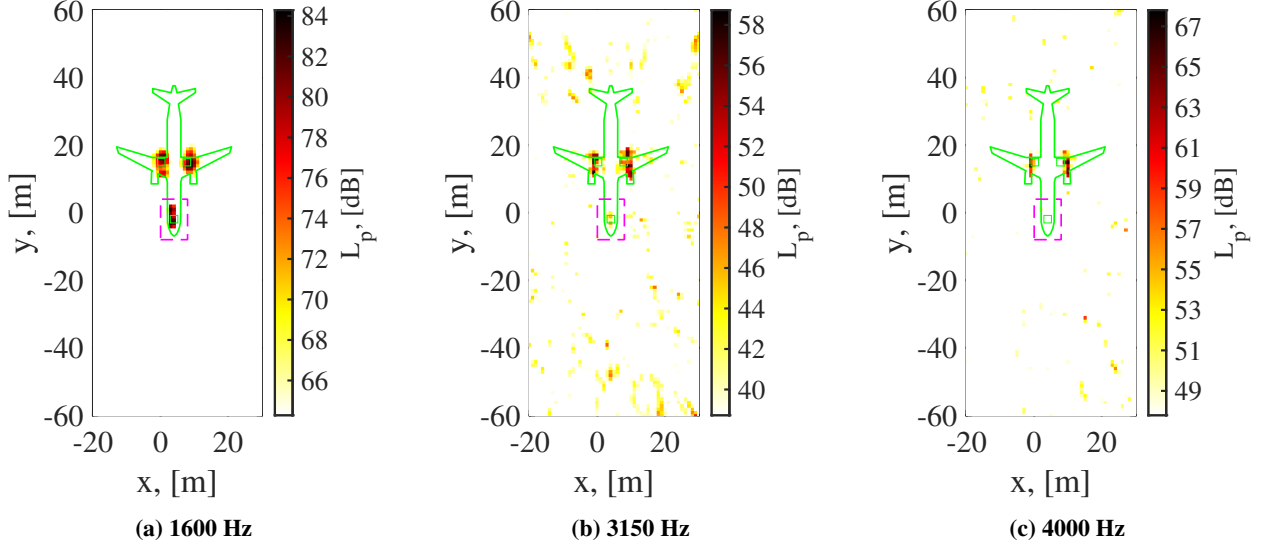**Fig. 8   Functional beamforming acoustic source plots for an Airbus A321 flyover with an aircraft velocity overhead of $V = 73.6$ m/s for different one-third-octave frequency bands. The aircraft silhouette is depicted as a green line with the landing gear wheels denoted with squares.**

now more shifted towards the MLG but, unfortunately, it is once again not possible to confirm this claim due to the insufficient spatial resolution of the microphone array at this frequency. In general, the peak levels in the acoustic source maps are approximately 3 dB, 4 dB, and 1 dB lower than the corresponding values for the A321*neo* depicted in Figs. 6 and 7. It also seems that for the *neo* case (Fig. 6(b)) the engines are relatively louder than the NLG at 1600 Hz, whereas for the *ceo* case (Fig. 8(a)) NLG and engines (and/or MLG) present similar noise levels. The relative prominence of the NLG tonal noise with respect to other (broadband) noise sources will condition the tonality values discussed later on in the psychoacoustic analysis of Sec. IV.B. These results are in agreement with the spectra comparison shown in Fig. 5(b), although, for a more accurate sound source quantification, integration techniques should be applied on the acoustic source maps[64].

A further analysis of the NLG tonal noise is presented in Fig. 9 where the tonal peak frequency f_{peak} and the respective peak sound pressure level values $L_{p,peak}$ (extracted from the single microphone spectra) at the overhead position are shown. Four flyovers (two A319, one A320*neo*, and one A321) presented no clear NLG tone at the overhead time and have been excluded from this figure. Even though the aircraft velocities V vary from approximately 60 to 78 m/s, the tonal peak frequency remains relatively constant around 1710 Hz (see Fig. 9(a)). Note that the frequency resolution in the spectrograms employed for the analysis is 10 Hz. The $L_{p,peak}$ values, on the other hand, present a relatively strong and significant correlation with the aircraft velocity, see Fig. 9(b), with a Pearson correlation coefficient ρ of 0.65 and a p-value of 2.5×10^{-5}. A scaling law for the acoustic power with an exponent of 12.6 for the aircraft velocity was found, which is in agreement with those reported in the literature [22, 65]. For similar aircraft velocity values, the *neo* aircraft seem to present higher $L_{p,peak}$ values compared to the rest of the aircraft analyzed.

B. Psychoacoustic analysis

The main results of the psychoacoustic analysis conducted for all the aircraft flyover recordings are presented in Fig. 10. Each subfigure corresponds to a different metric: (a) Effective Perceived Noise Level (EPNL), (b) Psychoacoustic Annoyance (PA), (c) Loudness (N_5), and (d) Tonality (K_5). In Fig. 10 the transparency of the marker fillings is indicative of the aircraft velocity, with a higher transparency corresponding to a lower velocity and vice versa. No significant correlation was found between any of the sound metrics and the aircraft velocity. This is in agreement with previous experimental studies analyzing the noise levels of other aircraft types [11]. For each metric, the mean values per aircraft subtype are denoted with a black marker.

In general, the EPNL, PA, and N_5 metrics present similar trends throughout the different aircraft subtypes. Overall, it seems that the *neo* versions are, on average, louder than their older *ceo* counterparts, with EPNL values approximately 3 EPNdB higher and PA values approximately 20% higher. The significance of these differences in the actual perceived
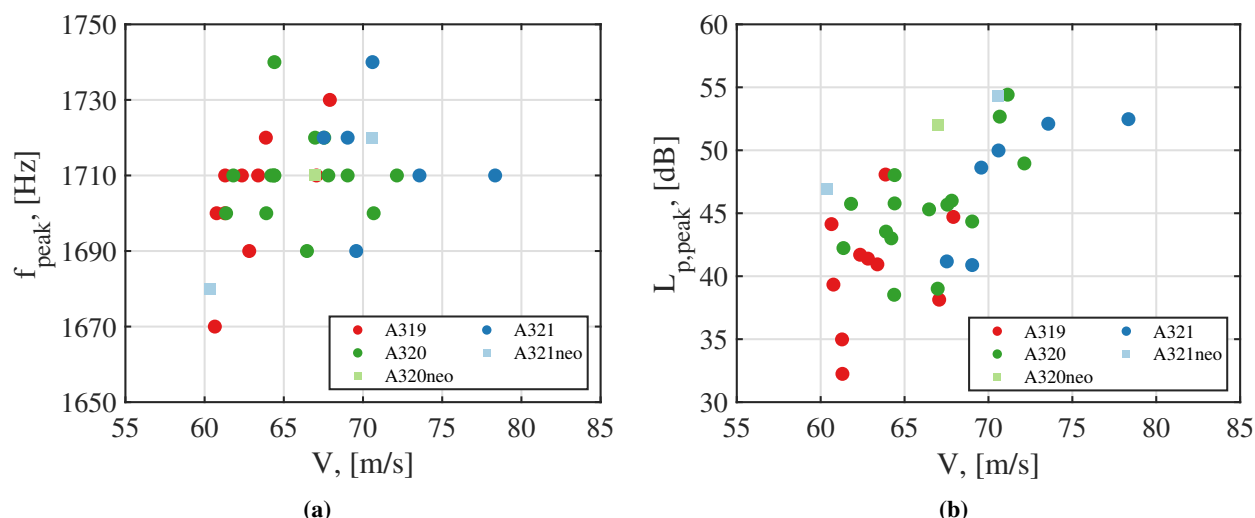
9

(a)　　　　　　　　　　　　　　　　　　　　　　　　　**(b)**

Fig. 9　(a) Peak tonal frequency and (b) corresponding sound pressure level $L_{p,peak}$ for the NLG noise at overhead position ($\theta \approx 90°$) versus the aircraft velocity overhead.

annoyance requires, however, experimental validation with listening experiments. These results contradict the lower number of complaints registered by the *neo* versions around AAS, see Fig. 1b. However, since only two aircraft flyovers were measured per *neo* subtype, it is difficult to draw any conclusion from this particular comparison with certainty. When comparing the different aircraft subtypes, it seems that the A319 and A321 emit the lowest noise levels, followed by the A320. Despite its larger size, MTOW, number of passengers, and maximum thrust (see Table 1), the average levels for the three aforementioned metrics for the A321 flyovers are lower than those corresponding to the A320. This is in agreement with the frequency spectra presented in Fig. 5 for both A320 and A321 examples.

The tonality metric, on the other hand, presents lower values for the *neo* versions relative to their *ceo* counterparts, see Fig. 10d. This could be partly explained by the higher broadband noise levels observed for the *neo* versions in Fig. 5, despite presenting comparable tonal noise levels for the NLG component around 1700 Hz, and, in general, higher $L_{p,peak}$ values for similar aircraft velocities, see Fig. 9(b). In general, higher broadband noise levels (as aforementioned when discussing the acoustic source maps) can mask the prominence of narrowband tones and make them appear "less tonal" [29]. In general, the larger aircraft (A320 and A321) seem to emit less tonal noise (on average) compared to the lighter A319. Despite the importance of tonality in sound perception [66], psychoacoustic annoyance is mainly influenced by loudness. Hence, the PA trend observed between aircraft subtypes (see Fig. 10b) is considerably similar to that of loudness (see Fig. 10c) and not to that of tonality (see Fig. 10d).

Lastly, the variation of the recorded EPNL and the PA metric depending on the year of the first flight of each aircraft are presented in Fig. 11. In general, no significant correlation is observed between the noise metrics and the year of the first flight for any of the aircraft subtypes, except for the A321*ceo* ($\rho = 0.81$, p-value = 0.026 for EPNL). However, given the limited number of samples (seven) and the fact that not all A321 aircraft considered were equipped with the exact same turbofan engine model, it is again difficult to draw any conclusions with certainty. Moreover, several other factors, such as the fan rotational speed [4, 11, 67, 68], also play an important role in the variation of the noise levels and, hence, the noise annoyance, are, however, not analyzed in this study.

V. Conclusions

The current paper presents a preliminary psychoacoustic analysis of the noise emissions from the Airbus A320 aircraft family and its nose landing gear (NLG) system. The study is based on experimental acoustic recordings under operational conditions conducted at Amsterdam Airport Schiphol.

As reported in previous literature, it was found that the NLG system is a dominant tonal noise source for all aircraft subtypes considered (A319, A320, A320*neo*, A321, and A321*neo*) around 1700 Hz. The tonal frequency was found to be relatively constant with respect to the aircraft velocity, but the magnitude of the NLG tonal peak is strongly correlated with it.
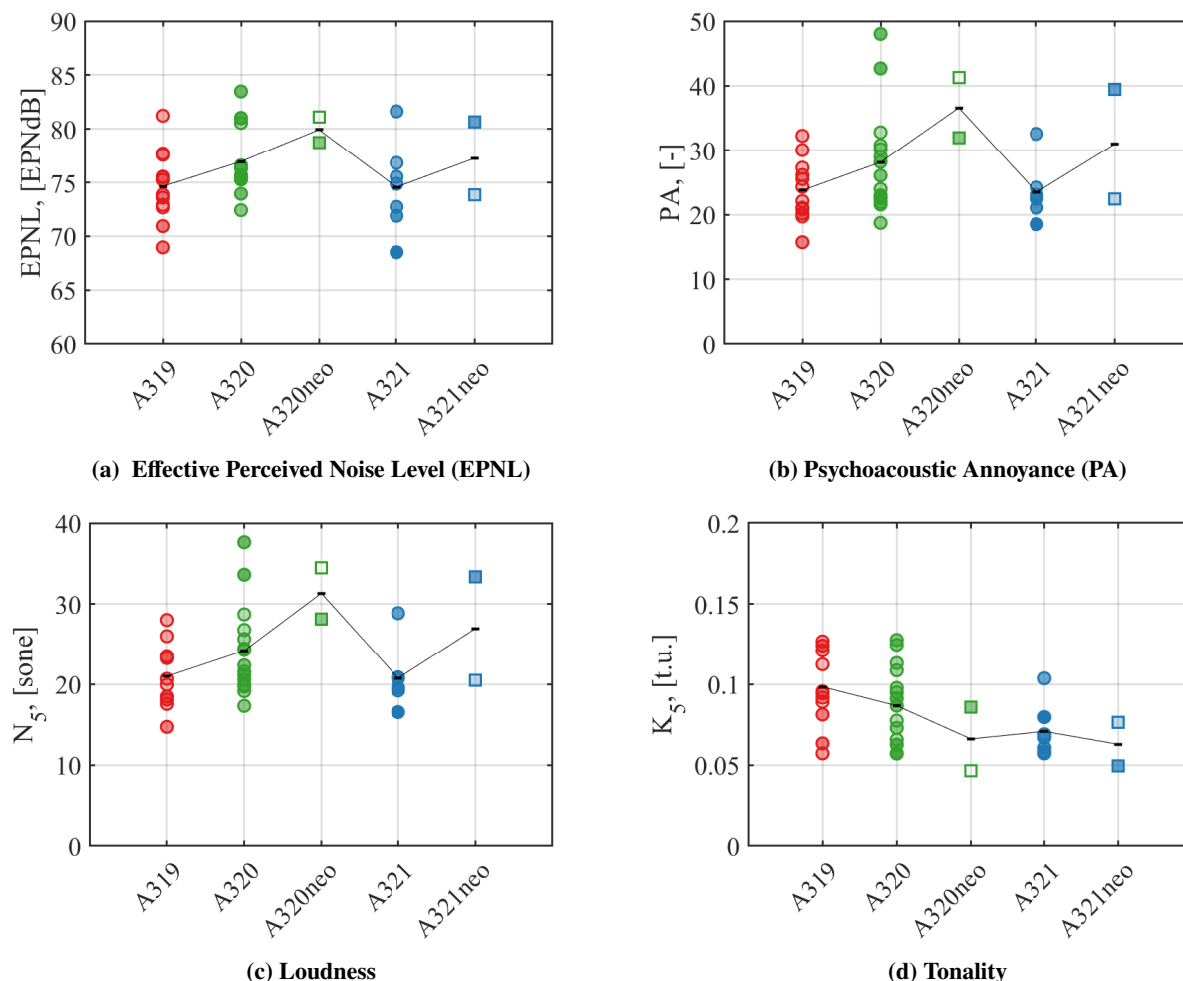
10

(a) Effective Perceived Noise Level (EPNL)

(b) Psychoacoustic Annoyance (PA)

(c) Loudness

(d) Tonality

Fig. 10 **Scatter plot for the measured (a) Effective Perceived Noise Level (EPNL), (b) Psychoacoustic Annoyance (PA), (c) Loundness (N_5), and (d) Tonality (K_5). The metrics are grouped per aircraft type, with the mean and trend line indicated in black. The transparency of the marker fill corresponds to the aircraft velocity; light/transparent fill indicates low values and vice versa.**

Regarding the expected psychoacoustic annoyance per aircraft subtype, the *neo* versions presented higher metric values for EPNL, PA, and loudness but lower tonality than their older *ceo* counterparts, providing contradicting results to the official noise assessment reports around the same airport. The lower tonality values for the *neo* versions are interesting despite presenting higher peak values for the NLG tone at similar aircraft velocities but could be partly explained by higher broadband noise masking the tones. However, given the low number of samples (only two A320*neo* and two A321*neo* flyovers were available), no strong conclusion can be drawn from this analysis. In addition, the acoustic measurements analyzed in this study were conducted very close to the runway threshold, where the operational and sound propagation conditions and, hence, noise footprints of these aircraft have different characteristics than at local communities around airports located further away. Therefore, a more extensive study featuring a higher number of *neo* flyovers and different observer positions is recommended for future work as the number of newer *neo* aircraft versions flying is expected to increase with time. In addition, the findings from the psychoacoustic analysis should also be confirmed in upcoming dedicated listening experiments with human listeners [69].
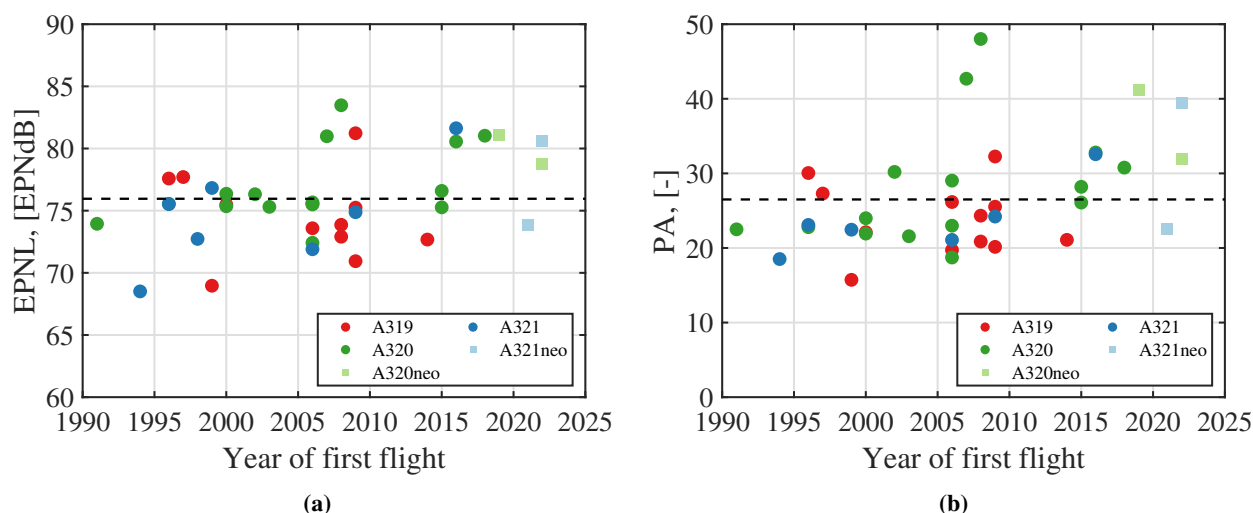
Fig. 11   Scatter plots for the (a) Effective Perceived Noise Level (EPNL) and (b) Psychoacoustic Annoyance (PA) values of each aircraft flyover ordered by the year of the first flight of each aircraft. The average values of the metrics for the entire dataset are marked with dotted black lines.

Acknowledgments

References

[1] Hansell, A., Blangiardo, M., Fortunato, L., Floud, S., de, H. K., Fecht, D., Ghosh, R., Laszlo, H., Pearson, C., Beale, L., Beevers, S., Gulliver, J., Best, N., Richardson, S., and Elliott, P., "Aircraft noise and cardiovascular disease near Heathrow airport in London: small area study," *British Medical Journal*, Vol. 347, 2013. https://doi.org/10.1136/bmj.f5432, URL http://dx.doi.org/10.1136/bmj.f5432.

[2] Organization, W. H., "Environmental Noise Guidelines for the European Region," Tech. Rep. ISBN 978-92-8-905356-3, World Health Organization. Regional Office for Europe, Copenhagen, Denmark, 2018. URL https://www.who.int/publications/i/item/9789289053563.

[3] Merino-Martinez, R., "Microphone arrays for imaging of aerospace noise sources," Ph.D. thesis, Delft University of Technology, 2018. https://doi.org/10.4233/uuid:a3231ea9-1380-44f4-9a93-dbbd9a26f1d6, URL https://repository.tudelft.nl/islandora/object/uuid:a3231ea9-1380-44f4-9a93-dbbd9a26f1d6?collection=research, ISBN: 978–94–028–1301–2.

[4] Merino-Martinez, R., Snellen, M., and Simons, D. G., "Calculation of the fan rotational speed based on flyover recordings for improving aircraft noise prediction models," 23rd *International Congress on Acoustics, September 9 – 13 2019, Aachen, Germany*, 2019. URL http://pub.dega-akustik.de/ICA2019/data/articles/000463.pdf.

[5] "ICAO Annex 16 Chapter 3. Environmental protection." Tech. rep., International Civil Aviation Organization (ICAO), Montreal, Canada, 2005.

[6] "Flightpath 2050 Europe's Vision for Aviation," Tech. rep., European Commission, 2012. https://doi.org/10.2777/50266, URL http://ec.europa.eu/transport/sites/transport/files/modes/air/doc/flightpath2050.pdf, ISBN: 978–92–79–19724–6.

[7] Casalino, D., Diozzi, F., Sannino, R., and Paonessa, A., "Aircraft noise reduction technologies: A bibliographic review," *Aerospace Science and Technology*, Vol. 12, No. 106705, 2008, pp. 1–17. https://doi.org/10.1016/j.ast.2007.10.004, URL https://www.sciencedirect.com/science/article/pii/S1270963807001162.

[8] Bertsch, L., "Noise Prediction within Conceptual Aircraft Design," Ph.D. thesis, DLR, Bunsenstrasse 10, 37073 Göttingen, Germany, 2013. URL http://elib.dlr.de/84386/1/phd_thesis_lothar_bertsch.pdf, DLR Forschungsbericht, ISRN DLR–FB–2013–20, ISSN 1434–8454.

[9] Dobrzynski, W., "Almost 40 Years of Airframe Noise Research: What Did We Achieve?" *Journal of Aircraft*, Vol. 47, No. 2, 2010, pp. 353–367. https://doi.org/10.2514/1.44457, URL http://arc.aiaa.org/doi/pdf/10.2514/1.44457.

[10] Merino-Martinez, R., Kennedy, J., and Bennett, G. J., "Experimental study of realisitic low–noise technologies applied to a full-scale nose landing gear," *Aerospace Science and Technology*, Vol. 113, No. 106705, 2021, pp. 1–20. https://doi.org/10.1016/j.ast.2021.106705, URL https://www.sciencedirect.com/science/article/pii/S1270963821002157?via%3Dihub.

[11] Merino-Martinez, R., Heblij, S. J., Bergmans, D. H. T., Snellen, M., and Simons, D. G., "Improving Aircraft Noise Predictions by Considering the Fan Rotational Speed," *Journal of Aircraft*, Vol. 56, No. 1, 2019, pp. 284–294. https://doi.org/10.2514/1.C034849, URL http://arc.aiaa.org/doi/abs/10.2514/1.C034849.

[12] Snellen, M., Merino-Martinez, R., and Simons, D. G., "Assessment of noise level variability on landing aircraft using a phased microphone array," *Journal of Aircraft*, Vol. 54, No. 6, 2017, pp. 2173–2183. https://doi.org/10.2514/1.C033950, URL http://dx.doi.org/10.2514/1.C033950.

[13] Merino-Martinez, R., Bertsch, L., Snellen, M., and Simons, D. G., "Analysis of landing gear noise during approach," 22nd *AIAA/CEAS Aeroacoustics Conference, May 30 – June 1 2016, Lyon, France*, 2016. https://doi.org/10.2514/6.2016-2769, URL http://arc.aiaa.org/doi/pdf/10.2514/6.2016-2769, AIAA paper 2016–2769.

[14] Merino-Martinez, R., Neri, E., Snellen, M., Kennedy, J., Simons, D. G., and Bennett, G. J., "Comparing flyover noise measurements to full–scale nose landing gear wind–tunnel experiments for regional aircraft," 23rd *AIAA/CEAS Aeroacoustics Conference, June 5 – 9 2017, Denver, Colorado, USA*, 2017. https://doi.org/10.2514/6.2017-3006, URL http://arc.aiaa.org/doi/pdf/10.2514/6.2017-3006, AIAA paper 2017–3006.

[15] Heller, H. H., and Dobrzynski, W. M., "Sound Radiation from Aircraft Wheel–Well/Landing–Gear Configuration," *Journal of Aircraft*, Vol. 14, No. 8, 1977, pp. 768–774. https://doi.org/10.2514/3.58851, URL http://arc.aiaa.org/doi/abs/10.2514/3.58851.

[16] Neri, E., Kennedy, J., and Bennett, G. J., "Bay cavity noise for full–scale nose landing gear: A comparison between experimental and numerical results," *Aerospace Science and Technology*, Vol. 72, 2018, pp. 278–291. https://doi.org/10.1016/j.ast.2017.11.016, URL https://doi.org/10.1016/j.ast.2017.11.016.

[17] Dobrzynski, W., Chow, L. C., Guion, P., and Shiells, D., "A European Study on Landing Gear Airframe Noise Sources," 6th *AIAA/CEAS Aeroacoustics Conference, June 12 – 14 2000, Lahaina, HI, USA*, 2000. https://doi.org/10.2514/6.2000-1971, URL http://arc.aiaa.org/doi/pdf/10.2514/6.2000-1971, AIAA paper 2000–1971.

[18] Merino-Martinez, R., Neri, E., Snellen, M., Kennedy, J., Simons, D. G., and Bennett, G. J., "Multi–approach study of nose landing gear noise," *Journal of Aircraft*, Vol. 57, No. 3, 2020, pp. 517–533. https://doi.org/10.2514/1.C035655, URL https://doi.org/10.2514/1.C035655.

[19] Michel, U., and Qiao, W., "Directivity of Landing–Gear Noise Based on Flyover Measurements," 5th *AIAA/CEAS Aeroacoustics Conference, May 10 – 12 1999, Bellevue, Greater Seattle, WA, USA*, 1999. https://doi.org/10.2514/6.1999-1956, URL http://dx.doi.org/10.2514/6.1999-1956, AIAA paper 1999–1956.

[20] Merino-Martinez, R., Snellen, M., and Simons, D. G., "Functional beamforming applied to imaging of flyover noise on landing aircraft," *Journal of Aircraft*, Vol. 53, No. 6, 2016, pp. 1830–1843. https://doi.org/10.2514/1.C033691, URL http://arc.aiaa.org/doi/abs/10.2514/1.C033691.

[21] Merino-Martinez, R., Neri, E., Snellen, M., Kennedy, J., Simons, D. G., and Bennett, G. J., "Analysis of nose landing gear noise comparing numerical computations, prediction models and flyover and wind–tunnel measurements," 24th *AIAA/CEAS Aeroacoustics Conference, June 25 – 29 2018, Atlanta, Georgia, USA*, 2018. https://doi.org/10.2514/6.2018-3299, URL http://arc.aiaa.org/doi/pdf/10.2514/6.2018-3299, AIAA paper 2018–3299.

[22] Merino-Martinez, R., and Snellen, M., "Implementation of tonal cavity noise estimations in landing gear noise prediction models," 26th *AIAA/CEAS Aeroacoustics Conference, June 15 – 19 2020, Virtual Event*, 2020. https://doi.org/10.2514/6.2020-2578, URL http://arc.aiaa.org/doi/pdf/10.2514/6.2020-2578, AIAA paper 2020–2578.

[23] Czech, M. J., Crouch, J. D., Stoker, R. W., Strelets, M. K., and Garbaruk, A., "Cavity noise generation for circular and rectangular vent holes," 12th *AIAA/CEAS Aeroacoustics Conference, May 8 – 10 2006, Cambridge, Massachusetts, USA*, 2006. https://doi.org/10.2514/6.2006-2508, URL http://arc.aiaa.org/doi/pdf/10.2514/6.2006-2508, AIAA paper 2006–2508.

[24] Pott-Pollenske, M., Dobrzynski, W., Buchholz, H., Gehlhar, B., and Walle, F., "Investigation of aircraft wake vortices with phased microphone arrays," 8th *AIAA/CEAS Aeroacoustics Conference, 17 – 19 June 2002, Breckenridge, Co, USA*, 2002. https://doi.org/10.2514/6.2002-2470, URL http://arc.aiaa.org/doi/abs/10.2514/6.2002-2470, AIAA paper 2002–2470.

[25] Pieren, R., Bertsch, L., Lauper, D., and Schäffer, B., "Improving future low–noise aircraft technologies using experimental perception–based evaluation of synthetic flyovers," *Science of the Total Environment*, Vol. 692, 2019, pp. 68–81. https://doi.org/10.1016/j.scitotenv.2019.07.253, URL https://doi.org/10.1016/j.scitotenv.2019.07.253.

[26] Fink, M. R., "Noise component method for airframe noise," 4*th* *AIAA Aeroacoustics Conference, October 3 – 5 1977, Atlanta, Georgia, USA*, 1977. https://doi.org/10.2514/6.1977-1271, URL http://arc.aiaa.org/doi/pdf/10.2514/6.1977-1271, AIAA paper 1977–1271.

[27] Guo, Y., "A Semi–Empirical Model for Aircraft Landing Gear Noise Prediction," 12*th* *AIAA/CEAS Aeroacoustics Conference, May 8 – 10 2006, Cambridge, Massachusetts, USA*, 2006. https://doi.org/10.2514/6.2006-2627, URL http://arc.aiaa.org/doi/pdf/10.2514/6.2006-2627, AIAA paper 2006–2627.

[28] Bertsch, L., Dobrzynski, W., and Guérin, S., "Tool Development for Low–Noise Aircraft Design," *Journal of Aircraft*, Vol. 47, No. 2, 2010, pp. 694–699. https://doi.org/10.2514/1.43188, URL http://arc.aiaa.org/doi/abs/10.2514/1.43188.

[29] Aures, W., "Procedure for calculating the sensory euphony of arbitrary sound signal. In German: Berechnungsverfahren für den sensorischen Wohlklang beliebiger Schallsignale," *Acustica*, Vol. 59, No. 2, 1985, pp. 130–141. URL https://www.ingentaconnect.com/contentone/dav/aaua/1985/00000059/00000002/art00008.

[30] Merino-Martinez, R., Vieira, A., Snellen, M., and Simons, D. G., "Sound quality metrics applied to aircraft components under operational conditions using a microphone array," 25*th* *AIAA/CEAS Aeroacoustics Conference, May 20 – 24 2019, Delft, The Netherlands*, 2019. https://doi.org/10.2514/6.2019-2513, URL http://arc.aiaa.org/doi/pdf/10.2514/6.2019-2513, AIAA paper 2019–2513.

[31] Vieira, A., Mehmood, U., Merino-Martinez, R., Snellen, M., and Simons, D. G., "Variability of sound quality metrics for different aircraft types during landing and take–off," 25*th* *AIAA/CEAS Aeroacoustics Conference, May 20 – 24 2019, Delft, The Netherlands*, 2019. https://doi.org/10.2514/6.2019-2512, URL http://arc.aiaa.org/doi/pdf/10.2514/6.2019-2512, AIAA paper 2019–2512.

[32] Merino-Martinez, R., Pieren, R., and Schäffer, B., "Holistic approach to wind turbine noise: From blade trailing–edge modifications to annoyance estimation," *Renewable and Sustainable Energy Reviews*, Vol. 148, No. 111285, 2021, pp. 1–14. https://doi.org/10.1016/j.rser.2021.111285, URL https://doi.org/10.1016/j.rser.2021.111285.

[33] Airbus, "Global Market Forecast – Flying by Numbers 2015–2034," Tech. Rep. D14029465, Airbus S.A.S., Blagnac, France, 2015. URL http://i2.cdn.turner.com/cnn/2015/images/09/02/global_market_forecast_2015-2034.pdf.

[34] Breugelmans, O., Houthuijs, D., van Poll, R., Hajema, K., and Hogenhuis, R., "Predicting aircraft noise annoyance: Exploring noise metrics other than Lden," 12*th* *ICBEN Congress on Noise as a Public Health Problem, June 12 – 18, Zurich, Switzerland*, 2017. URL http://www.icben.org/2017/ICBEN%202017%20Papers/SubjectArea08_Breugelmans_0802_3670.pdf.

[35] Kephalopoulos, S., Paviotti, M., Anfosso-Lédée, F., van Maercke, D., Shilton, S., and Jones, N., "Advances in the development of common noise assessment methods in Europe: The CNOSSOS–EU framework for strategic environmental noise mapping," *Science of the Total Environment*, Vol. 482–483, 2014, pp. 400–410. https://doi.org/10.1016/j.scitotenv.2014.02.031, URL https://doi.org/10.1016/j.scitotenv.2014.02.031.

[36] Bewoners Aanspreekpunt Schiphol, "BAS 2020 Jaarrapportage (in Dutch)," Tech. rep., Bewoners Aanspreekpunt Schiphol (BAS) (in English: Residents Contact Point Schiphol), 1118 ZG Schiphol, the Netherlands, Februari 2020. URL https://bezoekbas.nl/wp-content/uploads/2020/12/BAS-jaarrapportage-2020-inclusief-correctie-feb-2022.pdf.

[37] Bewoners Aanspreekpunt Schiphol, "BAS 2021 Jaarrapportage (in Dutch)," Tech. rep., Bewoners Aanspreekpunt Schiphol (BAS) (in English: Residents Contact Point Schiphol), 1118 ZG Schiphol, the Netherlands, Februari 2021. URL https://bezoekbas.nl/wp-content/uploads/2021/05/Jaarrapportage-BAS-2021.pdf.

[38] Bewoners Aanspreekpunt Schiphol, "BAS 2022 Jaarrapportage (in Dutch)," Tech. rep., Bewoners Aanspreekpunt Schiphol (BAS) (in English: Residents Contact Point Schiphol), 1118 ZG Schiphol, the Netherlands, Februari 2022. URL https://bezoekbas.nl/wp-content/uploads/2023/03/Bas-jaarrapport-2022-DEFINITIEF.pdf.

[39] Bewoners Aanspreekpunt Schiphol, "BAS 2023 Jaarrapportage (in Dutch)," Tech. rep., Bewoners Aanspreekpunt Schiphol (BAS) (in English: Residents Contact Point Schiphol), 1118 ZG Schiphol, the Netherlands, Februari 2023. URL https://bezoekbas.nl/wp-content/uploads/2023/04/BAS_Jaarrapportage_2023_DEF12042024.pdf.

[40] Greco, G. F., Merino-Martinez, R., Osses, A., and Langer, S. C., "SQAT: a MATLAB-based toolbox for quantitative sound quality analysis," 52th *International Congress and Exposition on Noise Control Engineering, August 20 – 23 2023, Chiba, Greater Tokyo, Japan*, ???? URL https://www.researchgate.net/publication/373334884_SQAT_a_MATLAB-based_toolbox_for_quantitative_sound_quality_analysis.

[41] Merino-Martinez, R., Pieren, R., Schäffer, B., and Simons, D. G., "Psychoacoustic model for predicting wind turbine noise annoyance," 24th *International Congress on Acoustics (ICA), October 24 – 28 2022, Gyeongju, South Korea*, 2022. URL https://www.researchgate.net/publication/364996997_Psychoacoustic_model_for_predicting_wind_turbine_noise_annoyance.

[42] EASA, "Data sheet for noise No. EASA.A.064.2 for Airbus A319," Tech. rep., European Union Aviation Safety Agency (EASA), 2 Rond-point Emile Dewoitine, 31700 Blagnac, France, February 2024. URL https://www.easa.europa.eu/en/downloads/8291/en.

[43] EASA, "Data sheet for noise No. EASA.A.064.3 for Airbus A320," Tech. rep., European Union Aviation Safety Agency (EASA), 2 Rond-point Emile Dewoitine, 31700 Blagnac, France, December 2023. URL https://www.easa.europa.eu/en/downloads/139012/en.

[44] EASA, "Data sheet for noise No. EASA.A.064.3 for Airbus A321," Tech. rep., European Union Aviation Safety Agency (EASA), 2 Rond-point Emile Dewoitine, 31700 Blagnac, France, March 2024. URL https://www.easa.europa.eu/en/downloads/120792/en.

[45] Greco, G. F. and Merino-Martinez, R. and Osses, A., "SQAT: a sound quality analysis toolbox for MATLAB (version v1.1),", May 2024. https://doi.org/10.5281/zenodo.10580337, URL https://zenodo.org/records/10580337, accessed in May 2024.

[46] Sijtsma, P., "Acoustic beamforming for the ranking of aircraft noise," Tech. Rep. NLR–TP–2012–137, National Aerospace Laboratory (NLR), Anthony Fokkerweg 2, 1059 CM Amsterdam, P.O. Box 90502, 1006 BM Amsterdam, The Netherlands, March 2012. URL https://reports.nlr.nl/xmlui/bitstream/handle/10921/482/TP-2012-137.pdf?sequence=1&isAllowed=y.

[47] Merino-Martinez, R., Luesutthiviboon, S., Zamponi, R., Rubio Carpio, A., Ragni, D., Sijtsma, P., Snellen, M., and Schram, C., "Assessment of the accuracy of microphone array methods for aeroacoustic measurements," *Journal of Sound and Vibration*, Vol. 470, No. 115176, 2020, pp. 1–24. https://doi.org/10.1016/j.jsv.2020.115176, URL https://doi.org/10.1016/j.jsv.2020.115176.

[48] PUI Audio POM–2735P–R microphone website, "http://www.puiaudio.com/product-detail.aspx?categoryId=4&partnumber=POM-2735P-R,", ???? URL http://www.puiaudio.com/product-detail.aspx?categoryId=4&partnumber=POM-2735P-R, accessed in January 2017.

[49] Flamex Basic – Acoustic Absorbing Foam, "https://www.akoestiekwinkel.nl/flamex?gclid=EAIaIQobChMI-bHpq5HA$_Q$IVWOd3Ch1wnwBYEAAYASA accessed in March 2017.

Airbus, Airbus A320 Aircraft Characteristics. Airport and Maintenance Planning, Tech. rep., Airbus S.A.S., Blagnac, France., 2005. `http://www.airbus.com/fileadmin/media_gallery/files/tech_data/AC/Airbus-AC_A320_01_May_2015.pdf`.

Schafer, M., Strohmeier, M., Lenders, V., Martinovic, I., and Wilhelm, M., Bringing up OpenSky: A large-scale ADS-B sensor network for research, *IPSN–14 Proceedings of the* 13th *International Symposium on Information Processing in Sensor Networks, April 15 – 17 2014, Berlin, Germany*, IEEE, 2014, pp. 83–94. 10.1109/IPSN.2014.6846743, `https://opensky-network.orghttp://ieeexplore.ieee.org/document/6846743/`.

Royal Netherlands Meteorological Institute (KNMI) website, https://www.knmi.nl/nederland-nu/klimatologie/uurgegeven, , ???? `https://www.knmi.nl/nederland-nu/klimatologie/uurgegeven`, accessed in August 2013.

Bergmans, D., Arntzen, M., and Lammen, W., Noise attenuation in varying atmospheric conditions, Tech. Rep. NLR–TP–2011–262, National Aerospace Laboratory (NLR), Anthony Fokkerweg 2, 1059 CM Amsterdam, P.O. Box 90502, 1006 BM Amsterdam, The Netherlands, November 2011. `https://reports.nlr.nl/xmlui/bitstream/handle/10921/129/TP-2011-262.pdf?sequence=1&isAllowed=y`.

ICAO Annex 16 – Environmental protection – Volume I – Aircraft Noise, Tech. Rep. AN 16–1, International Civil Aviation Organization (ICAO), Montreal, Canada, 2017. `https://store.icao.int/en/annex-16-environmental-protection-volume-i-aircraft-noise`.

Dougherty, R. P., Functional Beamforming, 5th *Berlin Beamforming Conference, February 19 – 20 2014, Berlin, Germany*, GFaI, e.V., Berlin, 2014. `http://bebec.eu/Downloads/BeBeC2014/Papers/BeBeC-2014-01.pdf`, BeBeC–2014–01.

Merino-Martinez, R., Snellen, M., and Simons, D. G., Functional Beamforming Applied to Full Scale Landing Aircraft, 6th *Berlin Beamforming Conference, February 29 – March 1 2016, Berlin, Germany*, GFaI, e.V., Berlin, 2016. `http://www.bebec.eu/Downloads/BeBeC2016/Papers/BeBeC-2016-D12.pdf`, BeBeC–2016–D12.

Welch, P. D., The Use of Fast Fourier Transform for the Estimation of Power Spectra: A Method Based on Time Averaging Over Short, Modified Periodograms, *IEEE Transactions on Audio and Electroacoustics*, Vol. AU–15, No. 2, 1967, pp. 70–73. 10.1109/TAU.1967.1161901, `http://ieeexplore.ieee.org/stamp/stamp.jsp?arnumber=1161901`.

ISO norm 532–1 – Acoustics – Method for calculating loudness – Zwicker method, Tech. Rep. 1, International Organization for Standardization, 2017. `https://www.iso.org/obp/ui/#iso:std:iso:532:-1:ed-1:v2:en`.

von Bismark, G., Sharpness as an attribute of the timbre of steady sounds, *Acta Acustica united with Acustica*, Vol. 30, No. 3, 1974, pp. 159–172. `https://www.semanticscholar.org/paper/Sharpness-as-an-attribute-of-the-timbre-of-steady-Bismarck/9576a2a74bff46ee0cded25bfd9e4302b4fb0470`.

Daniel, P., and Webber, R., Psychoacoustical Roughness: Implementation of an Optimized Model, *Accustica – acta acustica*, Vol. 83, 1997, pp. 113–123. `https://www.ingentaconnect.com/contentone/dav/aaua/1997/00000083/00000001/art00020`.

Osses, A., García León, R., and Kohlrausch, A., Modelling the sensation of fluctuation strength, 22nd *International Congress on Acoustics (ICA), September 5 – 9 2016, Buenos Aires, Argentina*, 2016. `https://pure.tue.nl/ws/portalfiles/portal/52366479/Osses_Garcia_Kohlrausch_ICA2016_ID113.pdf`.

Di, G.-Q., Chen, X.-W., Song, K., Zhou, B., and Pei, C.-M., Improvement of Zwicker's psychoacoustic annoyance model aiming at tonal noises, *Applied Acoustics*, Vol. 105, 2016, pp. 164–170. 10.1016/j.apacoust.2015.12.006, `http://dx.doi.org/10.1016/j.apacoust.2015.12.006`.

Greco, G. F. and Merino-Martinez, R. and Osses, A., SQAT: a sound quality analysis toolbox for MATLAB, , May 2023. `https://github.com/ggrecow/sqat`, accessed in May 2023.

Merino-Martinez, R., Sijtsma, P., Rubio Carpio, A., Zamponi, R., Luesutthiviboon, S., Malgoezar, A. M. N., Snellen, M., Schram, C., and Simons, D. G., Integration methods for distributed sound sources, *International Journal of Aeroacoustics*, Vol. 18, No. 4–5, 2019, pp. 444–469. 10.1177/1475472X19852945, `https://doi.org/10.1177/1475472X19852945`.

Ahuja, K. K., and Mendoza, J. M., Effects of Cavity Dimensions, Boundary Layer, and Temperature on Cavity Noise With Emphasis on Benchmark Data To Validate Computational Aeroacoustic Codes, Tech. Rep. NASA CR–4653, NASA, April 1995. `https://ntrs.nasa.gov/archive/nasa/casi.ntrs.nasa.gov/19950018459.pdf`.

Fastl, H., and Zwicker, E., *Psychoacoustics – Facts and models*, Third ed., Springer Series in Information Sciences, 2007. `https://www.springer.com/gp/book/9783540231592`, ISBN: 987–3–540–68888–4.

Snellen, M., Merino-Martinez, R., and Simons, D. G., Assessment of aircraft noise sources variability using an acoustic camera, 5th *CEAS Air & Space Conference, Challenges in European Aerospace, September 7 – 11 2015, Delft, Netherlands*, Council of European Aerospace Societies, Rue du Trone 98 – 1050 Brussels, Belgium, 2015. `http://repository.tudelft.nl/assets/uuid:d63eab6c-4cab-4ab2-ac14-d13d91837443/319502.pdf`.

Merino-Martinez, R., Snellen, M., and Simons, D. G., Determination of Aircraft Noise Variability Using an Acoustic Camera, 23rd *International Congress on Sound and Vibration, July 10 – 14 2016, Athens, Greece*, International Inst. of Acoustics and Vibration (IIAV), Auburn, Alabama, USA., 2016. `http://iiav.org/archives_icsv_last/2016_icsv23/content/papers/papers/full_paper_164_20160518160041692.pdf`.

Merino-Martinez, R., von den Hoff, B., and Simons, D. G., Design and acoustic characterization of a psychoacoustic listening facility, 29th *International Congress on Sound and Vibration (ICSV), July 9 – 13 2023, Prague, Czech Republic*, 2023. `https://www.researchgate.net/publication/372235624_Design_and_Acoustic_Characterization_of_a_Psychoacoustic_Listening_Facility`.

16